

This document contains a post-print version of the paper

## Digitally controlled electrorheological valves and their application in vehicle dampers

authored by **M. Kamelreiter, W. Kemmetmüller, and A. Kugi**  
and published in *Mechatronics*.

---

The content of this post-print version is identical to the published paper but without the publisher's final layout or copy editing. Please, scroll down for the article.

---

### Cite this article as:

M. Kamelreiter, W. Kemmetmüller, and A. Kugi, "Digitally controlled electrorheological valves and their application in vehicle dampers", *Mechatronics*, vol. 22, no. 5, pp. 629–638, 2012. DOI: [10.1016/j.mechatronics.2012.02.002](https://doi.org/10.1016/j.mechatronics.2012.02.002)

---

### BibTex entry:

```
% This file was created with JabRef 2.9.2.  
% Encoding: Cp1252
```

```
@ARTICLE{acinpaper,  
  author = {Kamelreiter, M. and Kemmetmüller, W. and Kugi, A.},  
  title = {Digitally controlled electrorheological valves and their application  
    in vehicle dampers},  
  journal = {Mechatronics},  
  year = {2012},  
  volume = {22},  
  pages = {629-638},  
  number = {5},  
  doi = {10.1016/j.mechatronics.2012.02.002},  
  url = {http://www.sciencedirect.com/science/article/pii/S0957415812000244}  
}
```

---

### Link to original paper:

<http://dx.doi.org/10.1016/j.mechatronics.2012.02.002>  
<http://www.sciencedirect.com/science/article/pii/S0957415812000244>

---

### Read more ACIN papers or get this document:

<http://www.acin.tuwien.ac.at/literature>

---

### Contact:

Automation and Control Institute (ACIN)  
Vienna University of Technology  
Gusshausstrasse 27-29/E376  
1040 Vienna, Austria

Internet: [www.acin.tuwien.ac.at](http://www.acin.tuwien.ac.at)  
E-mail: [office@acin.tuwien.ac.at](mailto:office@acin.tuwien.ac.at)  
Phone: +43 1 58801 37601  
Fax: +43 1 58801 37699

**Copyright notice:**

This is the authors' version of a work that was accepted for publication in *Mechatronics*. Changes resulting from the publishing process, such as peer review, editing, corrections, structural formatting, and other quality control mechanisms may not be reflected in this document. Changes may have been made to this work since it was submitted for publication. A definitive version was subsequently published in M. Kamelreiter, W. Kemmetmüller, and A. Kugi, "Digitally controlled electrorheological valves and their application in vehicle dampers", *Mechatronics*, vol. 22, no. 5, pp. 629–638, 2012. doi: [10.1016/j.mechatronics.2012.02.002](https://doi.org/10.1016/j.mechatronics.2012.02.002)

# Digitally Controlled Electrorheological Valves and their Application in Vehicle Dampers

Michael Kamelreiter<sup>a</sup>, Wolfgang Kemmetmüller<sup>a,\*</sup>, Andreas Kugi<sup>a</sup>

<sup>a</sup>Automation and Control Institute (ACIN), Vienna University of Technology, Gußhausstraße 27-29 / E376, 1040 Vienna, Austria

## Abstract

The idea to replace continuously adjustable proportional valves by a certain number of simple on/off valves is known as digital hydraulics. In recent years, various theoretical and practical works have shown the usefulness of this concept in classical hydraulics. This contribution is concerned with the application of the concept of digital hydraulics to electrorheological (ER) valves used in an ER damper. For this, a detailed mathematical model of ER valves, including the dynamics of the valve due to the inertia of the fluid, is developed. First of all, an ER damper based on conventional continuously adjustable ER valves is considered and its feasibility is proven by means of measurement results. In a second step, two constructions of digital ER valves are proposed which both are characterized by a very compact and simple design. The features of digital ER valves are analyzed by means of measurement results. Finally, the application of digital ER valves to an ER damper is shown and its properties are compared to the continuously adjustable ER damper in simulation studies on a validated model. It is shown that a similar high performance can be obtained with digital ER dampers at significantly lower overall system costs.

*Keywords:* electrorheological fluid, electrorheological damper, digital hydraulics, digital control

## 1. Introduction

Fast continuously adjustable servo or proportional valves are normally used in hydraulic applications with high demands on accuracy and bandwidth. In recent years, it has been shown that also electrorheological (ER) valves are well suited for active and semi-active applications with fast dynamics, see, e.g., [1] and [2] for servo drives, [3] and [4] for dampers and [5] for brakes. In conventional hydraulic valves, the volume flow is controlled by opening or closing an orifice by means of a spool. In an ER valve, in contrast, the volume flow is directly controlled by changing the apparent viscosity of the electrorheological fluid. This is done by applying a sufficiently large electric field to the ER fluid. Typically, the ER fluid is a suspension of polarizable particles in a fluid phase. Under the presence of an external electric field the particles form chains along the direction of the electric field, cf. [6], which cause the change of the apparent viscosity of the ER fluid. The ER effect is reversible, can be continuously controlled and exhibits a very fast response time in the range of a few milliseconds. The simple construction of ER valves using two electrodes which form a flat gap is a major advantage in comparison to conventional valves. There is, however, the need for an expensive linear high-voltage amplifier in

order to continuously adjust the volume flow through the ER valve.

A linear high-voltage amplifier can be replaced by a constant high voltage source, if instead of one continuously controlled ER valve several small digitally controlled ER valves are used, see [7]. The underlying idea is well known in conventional hydraulics [8] and was taken up again in 2001 by a group at Tampere University of Technology who proposed the name digital hydraulics, see [9]. The main idea of digital hydraulics is to use several adequately sized on/off valves in parallel instead of one proportional valve. In combination with a digital control strategy it is possible to adjust the volume flow of this digital valve over a wide range with sufficient accuracy. Feasibility and usefulness of this concept has been shown by means of practical applications, see, e.g., [9] and [10] for the position control of hydraulic cylinders. The benefits of digital hydraulics are low cost, robust valves, energy efficiency, fault tolerance, no spool position feedback and an amplitude-independent fast response time. In contrast to this there are a number of drawbacks in comparison to conventional proportional or servo valves, see, e.g., [9] and [11]: (i) Due to the finite number of on/off valves, a jerky motion can occur in hydraulic drives. (ii) Fast switching of the on/off valves causes pressure peaks in the system. (iii) Manufacturing tolerances and the different dynamics of the on/off valves can result in step uncertainties.

This contribution deals with the application of the idea of digital hydraulics to ER valves, see [7], and the practi-

\*Corresponding author.

Email addresses: [kamelreiter@acin.tuwien.ac.at](mailto:kamelreiter@acin.tuwien.ac.at) (Michael Kamelreiter), [kemmetmueller@acin.tuwien.ac.at](mailto:kemmetmueller@acin.tuwien.ac.at) (Wolfgang Kemmetmüller), [kugi@acin.tuwien.ac.at](mailto:kugi@acin.tuwien.ac.at) (Andreas Kugi)

cal application of digital ER valves in a vehicle damper, see also [12]. In this work, special emphasis is laid on the accurate modeling of the dynamics of the ER valve to assess the influence of the dynamics on the evolution of pressure peaks. The simple construction of an ER valve allows for the use of a higher number of on/off valves compared to conventional hydraulics. Furthermore, it is simpler to guarantee small manufacturing tolerances and the dynamics of ER valves is basically independent of the size. Finally, instead of using expensive linear high-voltage amplifiers, the high voltage only has to be switched on and off. This also significantly reduces the system costs.

The paper is organized as follows: Sections 2 and 3 are dedicated to the mathematical modeling of continuously adjustable ER valves and their application in a vehicle damper. Based on the model of the continuous ER valve, different constructions of digital ER valves are proposed and validated by means of measurement results in Section 4. In Section 5, the feasibility of the approach will be discussed by comparing the simulation results of a vehicle damper based on continuous ER valves with the same vehicle damper equipped with digital ER valves. Finally, in Section 6, a short summary and an outlook to future research activities are given.

## 2. Continuous ER valves

In this section, the mathematical model and the functional principle of a continuously adjustable ER valve are discussed. In general, an ER valve consists of a flat (or annular) channel of height  $H$ , which is formed by two electrodes of length  $L$  and width  $W$ , see Fig. 1. The pressure difference  $\Delta p = p_i - p_o$  between the inlet pressure  $p_i$  and the outlet pressure  $p_o$  drives a volume flow  $q$  of the ER fluid. By applying a voltage  $U$  to one electrode while the other electrode is earthed, an electric field  $E = U/H$  is generated which is used to change the rheological properties of the ER fluid.

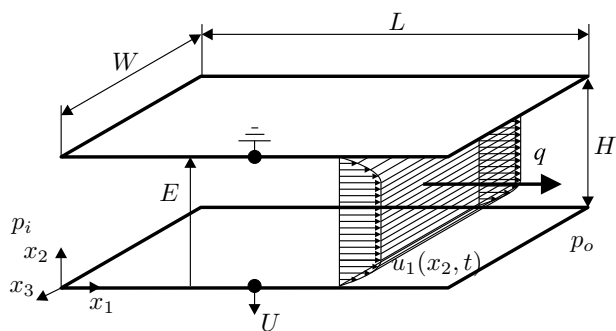


Figure 1: Flat channel ER valve.

In most cases the ER fluid is a suspension of polarizable particles in a fluid phase. In order to describe the behavior of the ER fluid in response to an electric field  $E$ , mathematical models describing the microscopical behavior of the particles have been developed, see, e. g., [6]

or [13]. These models are, however, not suitable for the modeling of an ER valve, since the computational effort is by far too high. Therefore, mathematical models of ER valves are commonly based on the description of the behavior of the ER fluid in the framework of continuum mechanics. Here, a generalized Cauchy stress tensor incorporating the electric field is employed, see, e. g., [14], [15]. The general constitutive equation for this Cauchy stress tensor can be simplified for the given flat channel geometry and the following assumptions: (i) the fluid is isotropic, incompressible and has a constant temperature, (ii) the flow in the ER valve is laminar and (iii) the dynamics of the ER effect can be neglected. Then, an extended Bingham material model of the form (see, e. g., [16])

$$\sigma_{12} = \tau_0(E)\text{sign}(\dot{\gamma}) + \eta\dot{\gamma} \quad \text{if } \dot{\gamma} \neq 0, \quad (1)$$

with the shear stress  $\sigma_{12}$ , the field strength dependent yield stress  $\tau_0(E)$ , the shear rate  $\dot{\gamma} = \partial u_1(x_2, t)/\partial x_2$ , the velocity profile  $u_1(x_2, t)$  and the dynamic viscosity  $\eta$  of the ER fluid for  $E = 0$ , can be derived. Based on measurements, the following relation is used for the approximation of  $\tau_0(E)$

$$\tau_0(E) = \begin{cases} a_1 E + a_2 E^2 + a_3 E^3 & \text{if } E < \bar{E} \\ b_0 + b_1 E & \text{else.} \end{cases} \quad (2)$$

Therein, the constant parameters  $a_1, a_2, a_3, b_0, b_1$  and  $\bar{E}$  are obtained from measurements, see Fig. 2 for the characteristic behavior of a typical ER fluid.

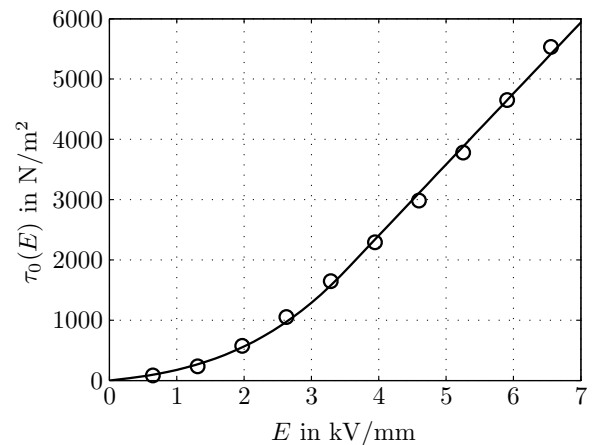


Figure 2: Comparison between model (solid line) and measurement (circles) of the field dependent yield stress  $\tau_0(E)$  of a typical ER fluid.

The practical applicability of devices based on digital ER valves depends essentially on the pressure peaks and/or volume flow peaks induced by the switching of the individual valves. In order to be able to describe the transient signals during switching, a dynamic model of the ER valve is needed. In general, ER valves exhibit a finite dynamics due to the following two reasons: (i) The ER effect,

i. e. the formation of particle chains, is not infinitely fast. Therefore, the static relationship (2) has to be extended by some kind of dynamics. (ii) The inertia of the ER fluid is not negligible, i. e. pressure drop and volume flow are coupled via a differential equation. In the literature, only a few works are dealing with the modeling of the dynamics of ER valves, see, e. g. [17] and [18]. In the following a brief summary of the model obtained by [17] will be given, considering the dynamics only due to the inertia of the fluid. This model will then be extended to cover at least approximately the finite dynamics of the ER effect.

The dynamic behavior of an ER fluid flowing through a flat channel ER valve is governed by the constitutive equation (1) and the balance of momentum

$$\rho \frac{\partial}{\partial t} u_1(x_2, t) = P(t) + \frac{\partial}{\partial x_2} \sigma_{12}(\dot{\gamma}, t), \quad (3)$$

with the pressure gradient  $P(t) = \Delta p(t)/L$ . Combining (1) and (3) leads to the inhomogeneous, parabolic partial differential equation

$$\frac{\partial}{\partial t} u_1(x_2, t) - \frac{\eta}{\rho} \frac{\partial^2}{\partial x_2^2} u_1(x_2, t) = \frac{1}{\rho} P(t). \quad (4)$$

By taking in mind that the velocity profile is symmetrical with respect to the middle of the gap, only the domain  $0 \leq x_2 \leq H/2$  has to be considered. The boundary conditions (BC) read as

$$\text{BC1: } u_1(0, t) = 0 \quad (5a)$$

$$\text{BC2: } \left. \frac{\partial}{\partial x_2} u_1(x_2, t) \right|_{x_2=H/2} = -\frac{\tau_0(t)}{\eta}, \quad (5b)$$

where (5a) is the non-slip condition at the electrode of the valve, (5b) describes the skew-symmetry of the stress in the valve, i. e.  $\sigma_{12}(H/2) = 0$ , and  $\tau_0(t) = \tau_0(E(t))$ . The initial condition (IC) of the velocity profile is assumed to be of the form

$$\text{IC: } u_1(x_2, 0) = u_{1,0}(x_2), \quad (6)$$

with

$$u_{1,0}(x_2) = \frac{P_0}{\eta} \frac{x_2}{2} (H - x_2) - \frac{\tau_{0,0}}{\eta} x_2 \quad (7)$$

which is the stationary solution of (4) and (5) for  $\tau_0(t) = \tau_{0,0}$  and  $P(t) = P_0$ , with given constant values of yield stress  $\tau_{0,0}$  and pressure gradient  $P_0$ . The general solution of (4), (5) and (6) takes the form [17]

$$u_1(x_2, t) = \bar{u}_1(x_2, t) + u_{1,0}(x_2) - \frac{\bar{\tau}_0(t)}{\eta} \frac{x_2^2}{H}, \quad (8)$$

with

$$\bar{u}_1(x_2, t) = \sum_{k=0}^{\infty} \frac{2}{\sqrt{H}} \sin\left((2k+1)\pi \frac{x_2}{H}\right) \bar{u}_{1,k}^*(t) \quad (9)$$

and

$$\bar{u}_{1,k}^*(t) = \int_0^t e^{-\frac{t-\lambda}{T_k}} \chi_k(\lambda) d\lambda. \quad (10)$$

Thereby, the time constants

$$T_k = \left( \frac{H}{(2k+1)\pi} \right)^2 \frac{\rho}{\eta}, \quad k = 0, 1, 2, \dots \quad (11)$$

and the quantities

$$\chi_k(t) = \frac{2\sqrt{H}}{\rho\pi(2k+1)} \bar{P}(t) - \frac{4}{\sqrt{H}\rho\pi(2k+1)} \bar{\tau}_0(t) + \frac{2H^{3/2}((-1)^k(2k+1)\pi - 2)}{(2k+1)^3\pi^3\eta} \frac{d}{dt} \bar{\tau}_0(t), \quad (12)$$

which are only depending on the inputs  $\bar{\tau}_0(t) = \tau_0(t) - \tau_{0,0}$  and  $\bar{P}(t) = P(t) - P_0$ , are used. The general solution (8) is only meaningful in the domain  $0 \leq x_2 \leq H_\gamma$ , where  $H_\gamma$  is the solution of

$$\left. \frac{\partial}{\partial x_2} u_1(x_2, t) \right|_{x_2=H_\gamma} = 0. \quad (13)$$

In the remainder of the domain a plug zone occurs, i. e. the fluid behaves in this region like a rigid body with the velocity profile

$$u_1(x_2, t) = u_1(H_\gamma, t), \quad H_\gamma < x_2 \leq H/2. \quad (14)$$

In order to get a better understanding of the dynamics, the result of the general solution (8), (14), for two different excitations will be investigated:

1. Stepwise change of the field dependent yield stress  $\tau_0(t)$  at a constant pressure gradient  $P(t)$ , i. e.

$$\bar{\tau}_0(t) = \bar{\tau}_0 \mathcal{H}(t) \quad (15a)$$

$$\bar{P}(t) = 0, \quad (15b)$$

with the step height  $\bar{\tau}_0$  and the Heaviside step function

$$\mathcal{H}(t) = \begin{cases} 0 & \text{for } t \leq 0 \\ 1 & \text{for } t > 0 \end{cases}. \quad (16)$$

2. Stepwise change of the pressure gradient  $P(t)$  at a constant yield stress  $\tau_0(t)$ , i. e.

$$\bar{\tau}_0(t) = 0 \quad (17a)$$

$$\bar{P}(t) = \bar{P} \mathcal{H}(t), \quad (17b)$$

with the step height  $\bar{P}$ .

The time evolution of the velocity profile for the two different excitations is depicted in Fig. 3 and Fig. 4. The velocity profile was calculated for the fluid parameters  $\eta = 27.4$  mPas and  $\rho = 1041$  kg/m<sup>3</sup>, the valve parameters  $H = 0.75$  mm,  $L = 70$  mm and  $W = 40$  mm and the infinite sum in (9) was approximated by a finite sum of 1000 elements. It can be seen in Fig. 3 that, starting from a parabolic velocity profile due to the absence of an electrical field, an increasing plug zone is occurring in the middle of the gap. Already after 8 ms the solution is close to the stationary velocity profile given by (7), (14). A very

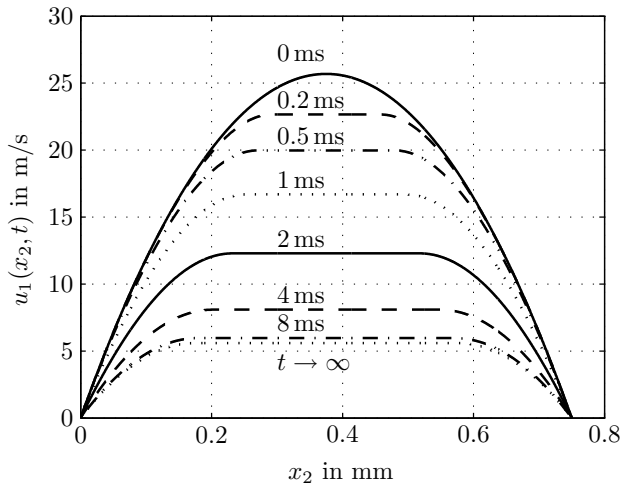


Figure 3: Transient behavior of the velocity profile  $u_1(x_2, t)$  for  $\tau_{0,0} = 0$ ,  $P_0 = \Delta p_0/L$  with  $\Delta p_0 = 7$  bar and a step in the yield stress of  $\bar{\tau}_0 = 2000$  N/m<sup>2</sup>.

similar dynamic behavior appears for the second scenario, where a step in the pressure gradient has been considered, see Fig. 4.

With regard to practical applications the dynamics of the volume flow  $q$  through the valve is more important than the dynamics of the velocity profile. The time evolution of  $q$  is obtained by integrating the velocity profile (8), (14) over the cross section of the valve. For the two excitations stated before we get the results illustrated in Fig. 5. Since the calculation of  $q$  based on (8) – (12) is rather time consuming and therefore not suitable for a controller design, an approximation of the dynamics of  $q$  by means of a Hammerstein-model [19] is proposed. The Hammerstein-model consists of a stationary input nonlinearity, which corresponds to the stationary volume flow relation

$$q_s(P, \tau_0) = \begin{cases} \frac{W(PH + \tau_0)(PH - 2\tau_0)^2}{12\eta P^2} & \text{if } \tau_0 \leq \frac{PH}{2} \\ 0 & \text{else,} \end{cases} \quad (18)$$

derived from (7), (14) for  $P_0 = P$  and  $\tau_{0,0} = \tau_0$ , and a linear time-invariant dynamic system connected in series

$$\dot{q} = -\frac{1}{T_0}(q - q_s(P, \tau_0)), \quad (19)$$

where  $T_0$  is the time constant according to (11) for  $k = 0$ . According to Fig. 5, there is an almost perfect agreement of the approximated model (18), (19) and the model from (8) – (12).

The dynamic model of the ER valve developed so far only incorporates the dynamics due to the inertia of the fluid. Next, this model is extended to be able to describe also the finite dynamics of the ER effect. Since the mathematical description of the ER effect on a particle level is by

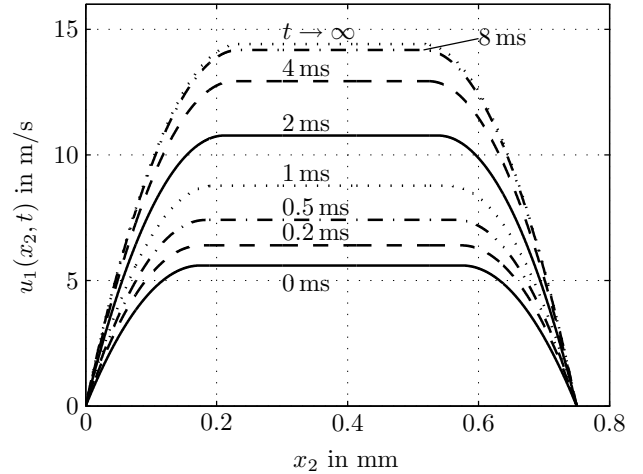


Figure 4: Transient behavior of the velocity profile  $u_1(x_2, t)$  for  $\tau_{0,0} = 2000$  N/m<sup>2</sup>,  $P_0 = \Delta p_0/L$  with  $\Delta p_0 = 7$  bar and a step in the pressure gradient of  $\bar{P} = \Delta \bar{p}/L$  with  $\Delta \bar{p} = 3$  bar.

far too complex to be used in this contribution, a heuristic model will be employed. Measurements have shown that the dynamics between the applied voltage  $U$  and the yield stress  $\tau_0$  can also be modeled by means of a Hammerstein-model. Here, the static input nonlinearity (2) is connected in series with the linear dynamics

$$\dot{\tau}_{0,h} = -\frac{1}{T_{er}}(\tau_{0,h} - \tau_0(U/H)), \quad (20)$$

where  $T_{er}$  is the time constant obtained by measurements. Thus, the overall dynamic model of an ER valve consists of two Hammerstein-models as depicted in Fig. 6, whereby  $s$  denotes the Laplace variable. This model will be used throughout this paper, whenever time domain simulations are carried out.

In the subsequent sections, the solution of the stationary volume flow (18) with respect to  $P$  is required. Inverting (18) for  $q_s = q > 0$  yields the pressure gradient

$$P = \underbrace{\frac{12\eta}{WH^3}q}_{P_N} + \underbrace{\frac{3\tau_0}{H} + 2A(\cos(\frac{1}{3}\arccos(1 - \frac{2\tau_0^3}{H^3A^3})) - 1)}_{P_U}, \quad (21)$$

with  $A = (WH^2\tau_0 + 4\eta q)/(WH^3)$ . Here,  $P_N$  is the pressure gradient for  $U = 0$  (Newtonian part) and  $P_U$  is the pressure gradient which can be controlled via the applied voltage  $U$ , with the property  $P_U = 0$  for  $U = 0$ . Thus, the stationary pressure drop along the ER valve reads as

$$\Delta p = (P_N + P_U)L. \quad (22)$$

In Fig. 7, the pressure-volume flow characteristics of an ER valve of the same size as before ( $H = 0.75$  mm,  $L = 70$  mm,  $W = 40$  mm) is given as a function of the applied voltage

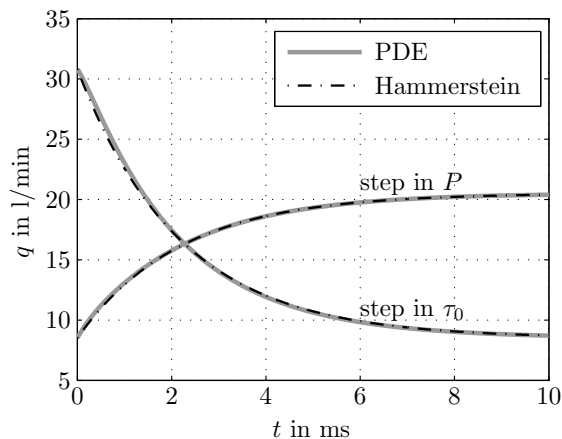


Figure 5: Comparison of the exact model from PDE and approximated Hammerstein-model of the volume flow through an ER valve due to a step in the pressure gradient and the yield stress.

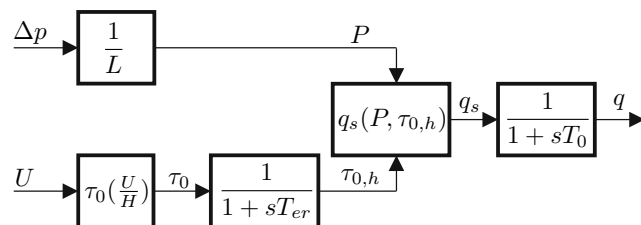


Figure 6: Block diagram of the dynamic model of an ER valve.

$U \in [0, U_{max}]$ , where  $U_{max} = 4\text{ kV}$  is the maximum voltage. The overall work space of the continuously adjustable ER valve is given by the grey shaded area.

### 3. Continuous ER damper

The ER damper prototype considered in this work together with the schematics for the use of continuous and digital ER valves is depicted in Fig. 8. The damper was designed by Fludicon GmbH, Darmstadt, Germany to be employed in a panel van with a gross vehicle weight of 3.5 t [12], [20]. The damper consists of 2 chambers with corresponding pressures  $p_1$  and  $p_2$  and effective piston areas  $A_1$  and  $A_2$ . For the gas pressure  $p_g$  of the piston type accumulator the approximation  $p_g \approx p_2$  will be used, since the accumulator piston mass is small and from measurements the friction force is known to be small, too. The chambers of the damper are connected via two ER valves and one check valve. During rebound of the damper the check valve is closed and hence both ER valves are connected in series. On the other hand, during compression the check valve is open and thus the volume flow only passes through the first ER valve. This construction leads to an asymmetrical characteristics of the controllable damping force, i. e.,

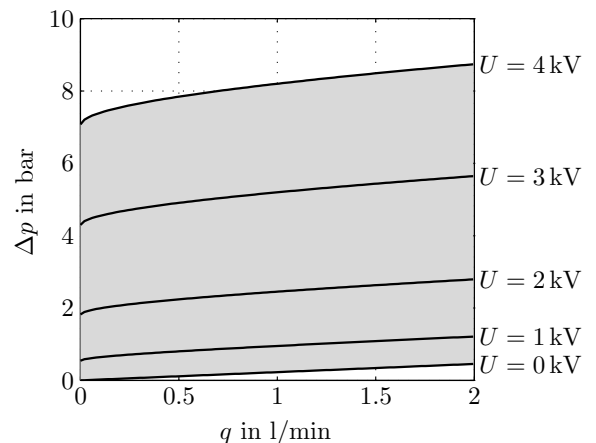


Figure 7: Characteristics of a continuously adjustable ER valve.

high damping in the rebound stage and low damping in the compression stage, which is typically used in automotive dampers to allow for a trade-off between ride comfort and road holding. The remaining quantities depicted in Fig. 8 are the piston displacement  $s$ , the piston velocity  $v$ , the pressure in between the ER valves  $p_3$ , the volume flows  $q_1$ ,  $q_2$  and  $q_3$  through the individual valves and the digital control inputs  $z_1$  and  $z_2$  which will be explained in the following sections.

By neglecting all the dynamics, i. e. assuming an incompressible fluid and infinitely fast ER valves ( $T_0 = 0$  and  $T_{er} = 0$ ), the force provided by the ER damper

$$F = F(s, v, U) = \underbrace{-(A_2 - A_1)p_2(s)}_{F_s(s)} + \underbrace{A_1 \Delta p(v, U)}_{F_d(v, U)} \quad (23)$$

with  $\Delta p = p_1 - p_2$  can be divided into an energy preserving spring part  $F_s(s)$  due to the gas-pressure in the accumulator and a dissipative damping part  $F_d(v, U)$  resulting from the pressure drop along the valves, see [20]. Friction forces between cylinder and piston are typically small compared to  $F_s(s)$  and  $F_d(v, U)$  and can therefore be neglected. The dissipative part of the considered continuously adjustable ER damper is depicted in Fig. 9 as a function of the voltage  $U$  applied to the ER valves. The forces during compression are plotted in the fourth quadrant in order to keep the illustration compact.

In order to validate the damper model, measurements have been carried out at a damper test stand. The goal was to track a desired trajectory of the damping force while the piston was moving in a sinusoidal way according to  $s = 0.04\sin(\pi t)$ . The control law necessary for this application, i. e. the applied voltage  $U$  as a function of the desired damping force  $F_d^d$  and the piston velocity  $v$ , can be obtained by inverting the dissipative part in (23) in the form

$$U = U(v, F_d^d). \quad (24)$$

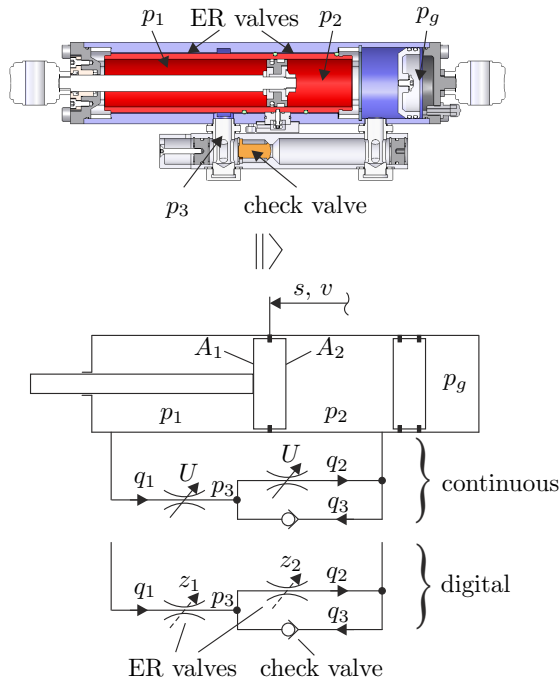


Figure 8: ER damper with schematics for the use of continuous and digital ER valves.

The results obtained at the damper test stand are depicted in Fig. 10. The measured damping force shows good agreement with its reference value and this justifies the feasibility of the mathematical models being used. The next sections will answer the question, whether and how it is possible to obtain similar results for the same ER damper but with digitally controlled ER valves.

#### 4. Digital ER valves

As already outlined in the introduction, the main idea of digital hydraulics is to approximate the functionality of continuously adjustable proportional valves by a number of independently controllable on/off valves. For this purpose,  $n$  on/off valves are typically connected in parallel, cf. Fig. 11. The overall volume flow of the digital valve is then given by

$$q = \sum_{j=1}^n q_j (\Delta p) s_j, \quad (25)$$

where  $s_j \in \{0, 1\}$  indicates if the corresponding valve is open or closed. By a suitable choice of the size (i. e. the effective opening area) of the valves it is possible to cover a wide volume range by a small number of valves. If a binary coding of the size of the valves is chosen, then the volume flows of the individual valves read as

$$q_j = q_B 2^{j-1}, \quad j = 1, \dots, n, \quad (26)$$

where  $q_B$  denotes the volume flow of the smallest valve. In conventional hydraulics, the main difficulties in designing

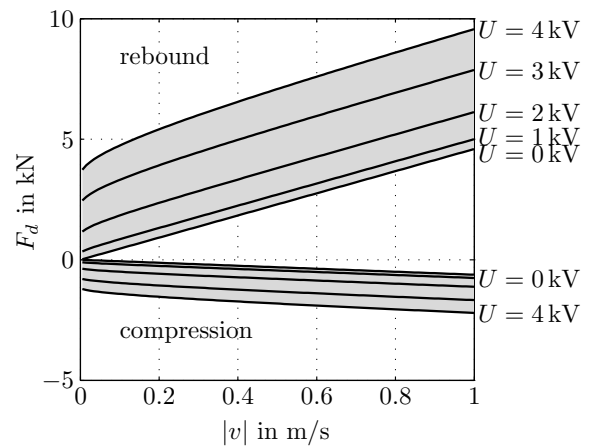


Figure 9: Characteristics of the continuously adjustable ER damper.

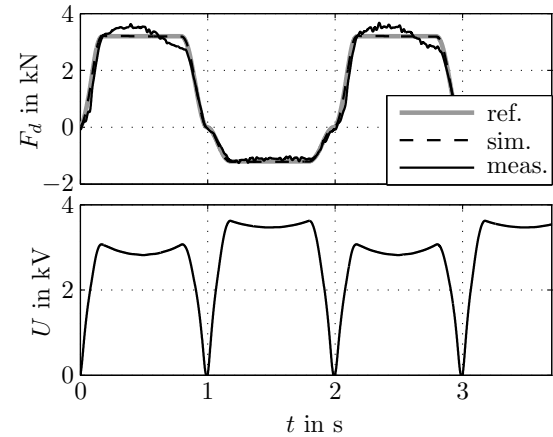


Figure 10: Comparison of measurement and simulation of a continuously adjustable ER damper.

such a digital valve are the high demands on the manufacturing accuracy and the timing of the valves.

The application of this idea to ER valves is straightforward since the volume flow (18) of an ER valve is a linear function of the valve's width  $W$ . Thus, it is only necessary to scale the widths of the individual ER valves according to

$$W_j = W_B 2^{j-1}, \quad j = 1, \dots, n, \quad (27)$$

with the width  $W_B$  of the smallest valve. Figure 12 depicts a possible construction of a parallel digital ER valve with  $n = 3$  bits. The control of these ER valves is carried out in the form  $U_j = (1 - s_j)U_{max}$ , with the constant voltage  $U_{max}$  and the switches (transistors)  $s_j \in \{0, 1\}$ ,  $j = 1, \dots, n$ . The overall volume flow through the parallel digital ER valve reads as

$$q = z q_B, \quad \text{with } z = \sum_{j=1}^n s_j 2^{j-1}, \quad (28)$$

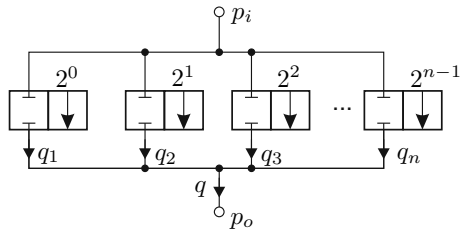


Figure 11: Basic concept of digital hydraulics.

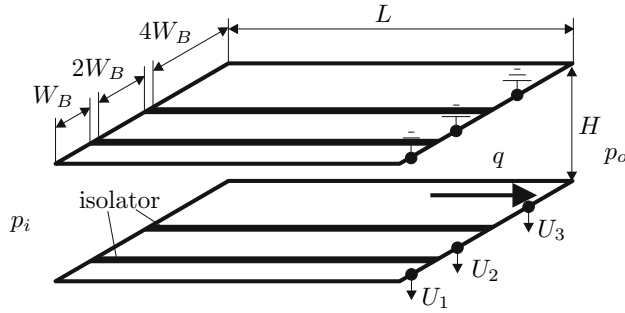


Figure 12: Configuration of a binary coded 3 bit parallel digital ER valve.

where  $q_B$  is the volume flow of the ER valve with the smallest width  $W_B$  and no voltage applied to it. Special attention has to be paid to the dimensioning of the length  $L$  and the height  $H$  of the individual valves. For a proper operation of the digital ER valve, it has to be guaranteed that the individual ER valves can be completely closed for the maximum expected pressure difference  $\Delta p_{max}$  if they are connected to the supply voltage  $U_{max}$ . This leads to the condition, cf. (18),

$$\Delta p_{max} \leq \frac{2L\tau_0(E_{max})}{H}, \quad \text{with} \quad E_{max} = \frac{U_{max}}{H} \quad (29)$$

for the choice of  $L$  and  $H$ .

Fig. 13 shows the pressure-volume flow relationship for a digital ER valve comprising 3 binary coded ER valves connected in parallel of height  $H = 0.75$  mm, length  $L = 70$  mm and width  $W_B = 5.7$  mm. It can be seen that the volume flow  $q$  through the digital ER valve can be controlled by switching on and off the voltages  $U_j$ ,  $j = 1, 2, 3$ , of the individual ER valves. The main advantages of a digital ER valve in comparison to digital hydraulics using conventional valves are: (i) The construction of the individual ER valves is very simple. Thus, it is easier to guarantee the necessary manufacturing accuracy. (ii) The individual ER valves can be included in one flat (or annular) channel by simply adjusting the areas of the electrodes. (iii) The dynamics of ER valves is independent of the width and length of the valves, cf. (11).

In many applications, e.g., semi-active dampers, it is desired to control the pressure drop along the valve rather than the volume flow through the valve, see, e.g., [21], [22], and [20]. Achieving this functionality with digital

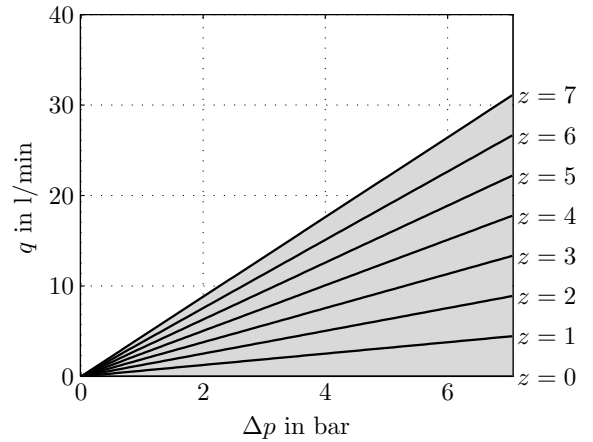


Figure 13: Characteristics of a binary coded 3 bit parallel digital ER valve.

hydraulics based on conventional on/off valves is difficult. In contrast, the pressure drop along a digitally controlled ER valve can be easily changed by switching on and off the applied voltage. Note that the pressure drop  $\Delta p$  along the ER valve for a constant voltage  $U$  and a constant volume flow  $q$  is a linear function of the length  $L$  of the valve, cf. (21) and (22). Thus, using  $n$  ER valves of height  $H$ , width  $W$ , and length

$$L_j = L_B 2^{j-1}, \quad j = 1, \dots, n, \quad (30)$$

where  $L_B$  denotes the length of the smallest valve, in series connection, a digital ER valve can be constructed which is very well suited for pressure control. The overall pressure drop along the serial digital ER valve is then given by

$$\Delta p = z\Delta p_B + \Delta p_N, \quad \text{with} \quad z = \sum_{j=1}^n s_j 2^{j-1}, \quad (31)$$

where  $\Delta p_N = P_N L$  is the overall Newtonian pressure drop with the overall length  $L = \sum L_j$  and  $\Delta p_B = P_U L_B$  is the pressure drop along the smallest valve without its Newtonian part for  $U = U_{max}$ .

Fig. 14 shows a possible implementation of a binary coded serial digital ER valve with 3 bit. The corresponding pressure-volume flow characteristics of a valve with  $H = 0.75$  mm,  $W = 40$  mm and  $L_B = 10$  mm is given in Fig. 15. This figure shows that a control of the pressure drop along the serial digital ER valve as a function of  $z$  is possible by switching on and off the voltage applied to the individual valves. The benefit of serial digital ER valves can be clearly seen by having a closer look at the characteristic curves for constant  $z$ , where only a small dependence of the pressure drop on the volume flow is given. Thus, even large changes in the volume flow lead to small changes in the pressure drop along the valve.

Up to now, a binary coding of the individual valves with size ratios of  $2^{j-1}$  has been used, since this yields

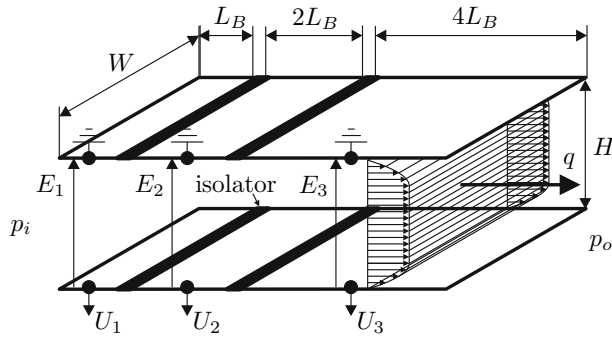


Figure 14: Configuration of a binary coded 3 bit serial digital ER valve.

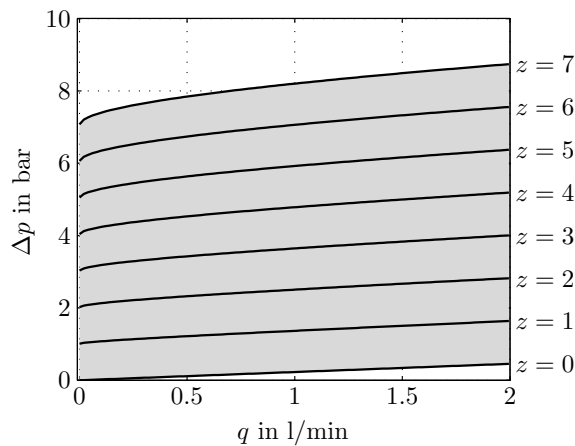


Figure 15: Characteristics of a binary coded 3 bit serial digital ER valve.

the lowest possible number of valves for a given resolution. However, since it is necessary to switch many valves at the same time in this coding scheme, e.g. when changing from state  $z = 7$  to  $z = 8$ , unequal dynamics of the valves and non-ideal flow rates (e.g. due to manufacturing tolerances) might lead to pressure peaks and nonlinear characteristics. In order to circumvent these drawbacks, different coding schemes have been outlined in the literature for conventional digital hydraulics. According to [11], pulse number modulation with equal size of all valves has the best properties in this context whereas coding based on the Fibonacci numbers with ratios 1, 1, 2, 3, 5, 8, ... and other hybrid schemes represent a middle course. In any coding scheme, the improvement of robustness is achieved by increasing the number of valves.

In general, the problems due to unequal valve rise times and non-ideal flow rates are less serious when using ER valves instead of conventional valves. As already mentioned, the construction of ER valves is very simple and hence a very accurate manufacturing can be expected. Secondly, the dynamics of ER valves only depend on the oil density, oil viscosity and the height of the valve, cf. (11). Thus, the dynamics is expected to be identical for parallel

or serial connected ER valves of different lengths or widths. However, if it is desired to use pulse number modulation due to its robustness, a large number of small and cheap valves is needed. ER valves are very well suited for this kind of application, since a large number of valves can be easily obtained by a suitable design of the electrodes of the valves. Despite the large number of valves, the construction and the control unit remain simple and thus costs are expected to be low.

In order to show the feasibility of digitally controlled ER valves, a test stand has been developed, see Fig. 16a. The test stand has two main features: (i) In addition to the measurement of the pressure drop, the volume flow, the voltage and the temperature, it is of great interest to examine the flow pattern within the ER valve. This requirement led to the use of optical transparent top and bottom walls (quartz glass) of the flat channel. By sputtering indium-tin-oxide (ITO) onto the glass surface, highly conductible electrodes of almost arbitrary shape and with a high optical transmittance can be produced. Fig. 16b shows the upper and lower electrode of a binary coded 3 bit serial digital ER valve. (ii) It is desired to test different configurations of serial or parallel digital ER valves with different shapes of the electrodes. This can be easily achieved by changing the two glass discs with the electrodes sputtered on.

In the subsequent measurements a binary coded 3 bit serial digital ER valve as depicted in Fig. 14 and Fig. 16b with a height  $H = 0.75$  mm, a width  $W = 40$  mm and a length  $L_B = 10$  mm is considered. For the validation of the 3 bit serial digital ER valve, static and dynamic measurements were carried out. The measured (static) pressure-volume flow characteristics in Fig. 17a show a very good agreement with the mathematical model for moderate and high volume flows. In the case of very low volume flows, however, larger deviations occur. This is due to the fact that the constitutive equation (1) is not able to exactly describe the behavior for small shear rates  $\dot{\gamma}$ . In practical applications, it is possible to avoid very low shear rates by means of a suitable construction of the valve. Furthermore, the static behavior can be approximated by look-up tables or more complex material models which are based on the measurement results. Nevertheless, the basic functionality of the serial digital ER valve could be demonstrated by the static measurement results.

To show the dynamic behavior of the serial digital ER valve a sinusoidal pressure signal is tracked with the digital ER valve at a constant volume flow of  $q = 2$  l/min. The results in Fig. 17b show again very good agreement of the measurements with the expected behavior. Especially, no pressure peaks during the switching of the valves could be observed which is in agreement with the theoretical examinations.

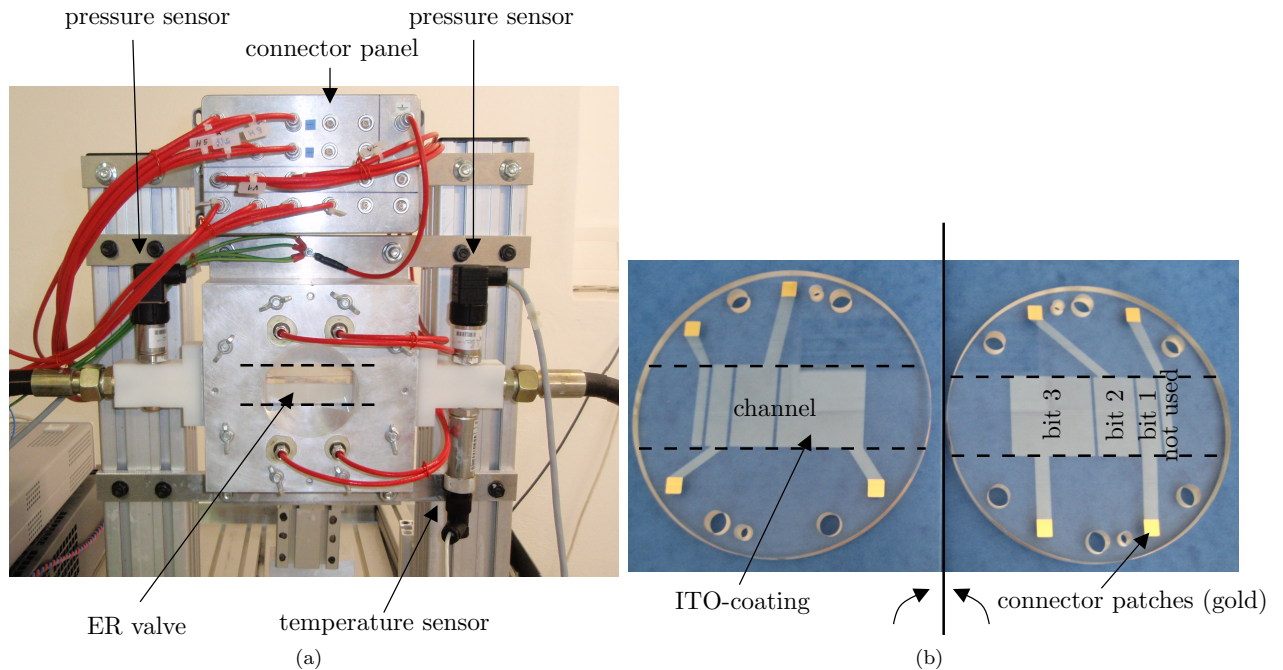


Figure 16: (a) ER valve test stand and (b) ITO coated glass discs.

### 5. Digital ER damper

The goal of this section is to show the feasibility of applications based on digitally controlled ER valves. Therefore, both continuous ER valves of the ER damper of Section 3 are replaced by adequately coded digital ER valves. Thereby, the overall dimensions of the digital valves are equal to the respective continuous valve, see Fig. 8. In the following, the ER valve with control input  $z_1$  and  $z_2$  will be denoted as first and second ER valve, respectively. The remaining degrees of freedom left for the construction of the digital ER damper are the choice of the coding scheme and the number of bits, for each of the two digital ER valves. An obvious solution, with a minimum number of ER valves, is a binary coding scheme for both valves. Unfortunately, this solution leads to a resolution which is different in the compression and the rebound stage. Furthermore, in the rebound stage the same force level can be obtained by different control inputs. By looking at the force difference between  $U = 0\text{ V}$  and  $U = 4\text{ kV}$  for  $|v| = 1\text{ m/s}$  in Fig. 9, it becomes obvious that the force difference in the rebound stage is about three times larger than in the compression stage. In other words, the pressure difference over the second ER valve is about twice the value of the first ER valve. This leads to the following choice of the coding for the two digital ER valves: To get a good force resolution in the compression phase at a minimum number of bits, a binary coding scheme with a resolution of  $n_1$  bits for the first ER valve will be used. The second ER valve will be coded linearly with  $n_2 = 2$  bit. Already a choice of  $n_1 = 3$  leads to a very good approximation of the damping characteristics of the continuous

ER damper, cf. Fig. 18.

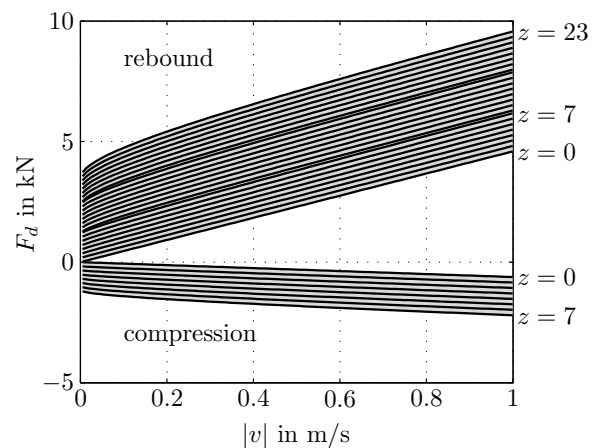


Figure 18: Characteristics of the proposed digital ER damper.

For a damping force control, the overall digital control input  $z$  as well as the partial control inputs  $z_1$  and  $z_2$  of the individual valves have to be calculated as a function of the desired damping force  $F_d^d$  and the piston velocity  $v$ . Again, for the controller design, the dynamics is neglected, i. e. an incompressible fluid and infinitely fast ER valves ( $T_0 = 0$  and  $T_{er} = 0$ ) are assumed. With these assumptions the overall pressure drop can be calculated as

$$\Delta p^d = p_1 - p_2 = \frac{F_d^d}{A_1} \quad (32)$$

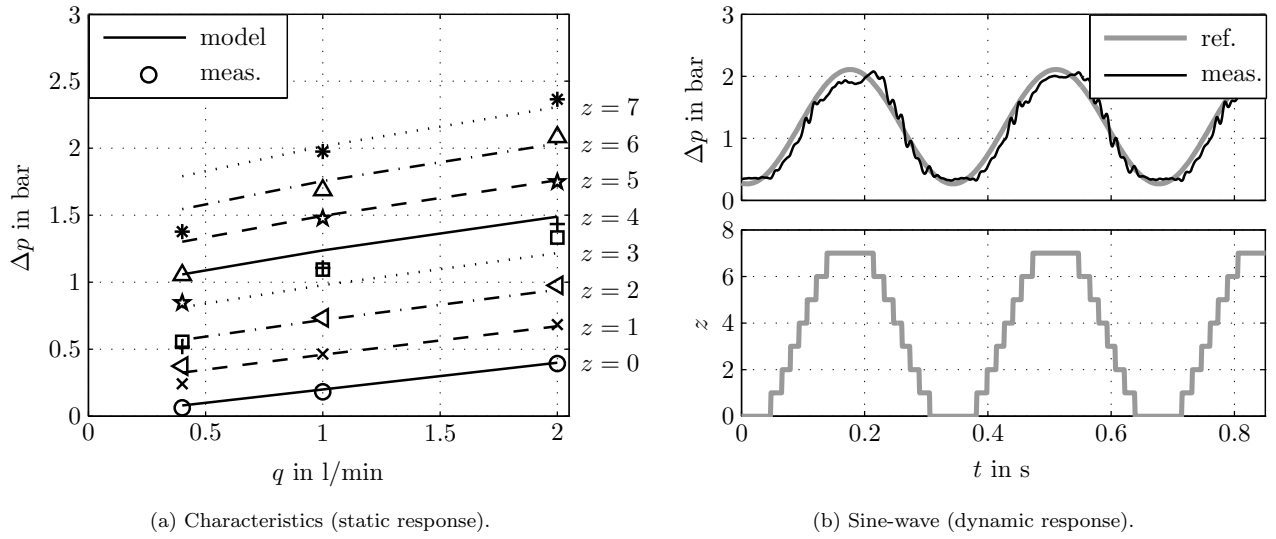


Figure 17: Comparison of measurement and model of a binary coded 3 bit serial digital ER valve.

and the volume flows are given by

$$q_1 = A_1 v \quad (33a)$$

$$q_2 = \begin{cases} A_1 v & \text{if } v > 0 \\ 0 & \text{if } v \leq 0. \end{cases} \quad (33b)$$

The pressure differences over the first ER valve  $\Delta p_1 = p_1 - p_3$  and the second ER valve  $\Delta p_2 = p_3 - p_2$  are given in the form

$$\Delta p_1 = \Delta p_{B1} z_1 + \Delta p_{N1} \quad (34a)$$

$$\Delta p_2 = \Delta p_{B2} z_2 + \Delta p_{N2}, \quad (34b)$$

with  $\Delta p_{B1} = P_U L_{B1}$ ,  $\Delta p_{N1} = P_N L_1$  and  $z_1 \in \{0, 1, \dots, 2^{n_1} - 1\}$  for the first binary coded valve and  $\Delta p_{B2} = P_U L_{B2}$ ,  $\Delta p_{N2} = P_N L_2$  and  $z_2 \in \{0, 1, \dots, n_2\}$  for the second linearly coded valve. Thereby, the overall length of the two ER valves is denoted by  $L_1$  and  $L_2$ , the respective length of the shortest valve is denoted by  $L_{B1}$  and  $L_{B2}$  and the pressure gradients  $P_N$  and  $P_U$  are given by (21). Subsequently it is assumed that the desired damping force can be realized and hence lies within the damping characteristics of the ER damper. Since the ER damper is a passive system which cannot actively generate any force at rest, we will additionally assume that  $F_d^d = 0$  holds for  $v = 0$ . Considering these assumptions, the partial control inputs  $z_1$  and  $z_2$  are given in the compression phase, i. e. for  $v \leq 0$ , by

$$z_1 = \left\lfloor \frac{\Delta p^d - \Delta p_{N1}}{\Delta p_{B1}} \right\rfloor \quad (35a)$$

$$z_2 = 0, \quad (35b)$$

and in the rebound phase, i. e. for  $v > 0$ , by

$$z_2 = \left\lfloor \frac{\Delta p^d - \Delta p_{N1} - \Delta p_{N2}}{\Delta p_{B2}} \right\rfloor \quad (36a)$$

$$z_1 = \left\lfloor \frac{\Delta p^d - \Delta p_{N1} - \Delta p_{N2} - z_2 \Delta p_{B2}}{\Delta p_{B1}} \right\rfloor, \quad (36b)$$

where  $\lfloor x \rfloor$  denotes the integer part of  $x$ . The overall control input then reads as

$$z = z_1 + 2^{n_1} z_2. \quad (37)$$

In order to assess the quality of the digital ER damper the tracking results for the same force trajectory as for the continuous ER damper are depicted in Fig. 19. Thereby, a dynamics of the ER effect of  $T_{er} = 1$  ms has been used. The simulation results show that the tracking performance of the digital ER damper is almost as good as the corresponding continuous version. It should be emphasized, that these excellent results are already obtained with a low resolution of 3 bit for the first and 2 bit for the second ER valve. Dynamical pressure or force peaks, which are known from conventional digital hydraulics, could not be observed. Therefore, digital ER valves are a very interesting approach for semi-active suspension systems, both with respect to their high performance and the low system costs

## 6. Conclusion and Outlook

In this paper, the idea of digital hydraulics was successfully extended and applied to an ER damper prototype. A dynamical model of continuously adjustable ER valves was presented, considering the inertia of the fluid and the dynamics of the ER effect, in order to assess the magnitude of

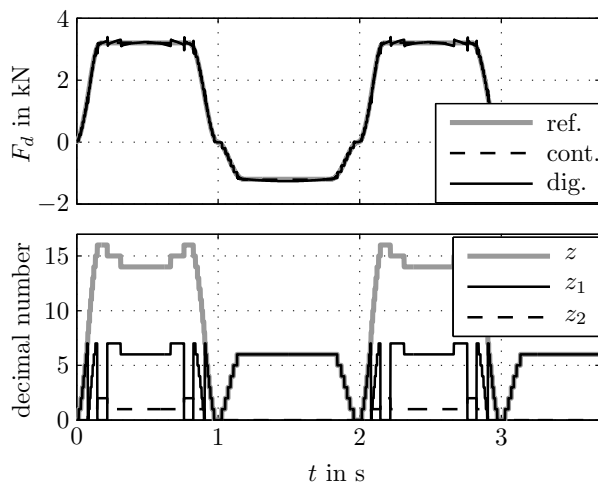


Figure 19: Comparison of the simulation results of the continuous and the digital ER damper.

pressure peaks induced by the switching of the ER valves. Simulation results of the model of an ER damper prototype using these continuously adjustable ER valves show good agreement with measured data recorded at a damper test stand. Based on the mathematical model of continuous ER valves, two different types of digital ER valves were introduced. A parallel connection of ER valves yields a good control of the volume flow while a serial connection of the individual ER valves permits the exact control of the pressure drop along the valve. Measurement results of a 3 bit serial digital ER valve on a test stand confirmed the results of the theoretical examinations and proved the feasibility of the proposed digital ER valves. Finally, the continuous ER valves of the ER damper prototype were replaced by adequately coded digital ER valves. In simulation, this digital damper shows only a marginal decrease of performance in comparison to the continuous version. Remarkably, this result can be achieved at lower system costs, since instead of a linear high voltage amplifier only a constant high voltage source is needed. System inherent problems often occurring in conventional digital hydraulic systems as e. g. pressure peaks and step size uncertainties, could be kept very small with the proposed digital ER valves. Further research will focus on the implementation of digital ER valves in semi-active suspension systems.

### Acknowledgment

The authors would like to thank Fludicon GmbH, Darmstadt, Germany, in particular Mr. M. Stork and Mr. K. Holzmann for the fruitful cooperation.

### References

- [1] S. Choi, M. Cho, Control performance of hydraulic servo valves utilising electrorheological fluids, *Journal of Vehicle Design* 38 (2/3) (2005) 196–209.

- [2] W. Kemmetmüller, A. Kugi, Modeling and control of an electrorheological actuator, in: *Proceedings of the 3rd IFAC Symposium on Mechatronic Systems*, Vol. 1, Sydney, Australia, 2004, pp. 265–270.
- [3] S. Choi, S. Han,  $H_\infty$  control of electrorheological suspension system subjected to parameter uncertainties, *Mechatronics* 13 (2003) 639–657.
- [4] A. Kugi, K. Holzmann, W. Kemmetmüller, Active and semi-active control of electrorheological fluid devices, in: H. Ulbrich, W. Günthner (Eds.), *IUTAM Symposium on Vibration Control of Nonlinear Mechanisms and Structures*, Dordrecht, The Netherlands, Springer, Munich, Germany, 2005, pp. 203–212.
- [5] K. Tan, R. Stanway, W. Bullough, Braking responses of inertia/load by using an electrorheological (ER) brake, *Mechatronics* 17 (2007) 277–289.
- [6] M. Parthasarathy, D. Klingenberg, Electrorheology: Mechanisms and models, *Journal of Material Science and Engineering R17* (1996) 57–103.
- [7] M. Kamelreiter, W. Kemmetmüller, A. Kugi, Digital control of electrorheological valves, in: *Proceedings of the 5th IFAC Symposium on Mechatronic Systems*, IFAC, Boston, USA, 2010.
- [8] F. Rickenberg, Valve. US1757059. (1930).
- [9] M. Linjama, A. Laamanen, M. Vilenius, Is it time for digital hydraulics?, in: *Proceedings of the Eighth Scandinavian International Conference on Fluid Power*, Tampere, Finland, 2003, pp. 347–366.
- [10] A. Laamanen, M. Linjama, M. Vilenius, On the pressure peak minimization in digital hydraulics, in: *Proceedings of the Tenth Scandinavian International Conference on Fluid Power*, Vol. 2, Tampere, Finland, 2007, pp. 107–122.
- [11] M. Linjama, M. Vilenius, Digital hydraulics - towards perfect valve technology, in: *Proceedings of the Tenth Scandinavian International Conference on Fluid Power*, Vol. 1, Tampere, Finland, 2007, pp. 181–196.
- [12] M. Kamelreiter, W. Kemmetmüller, A. Kugi, Digitale Ansteuerung elektrorheologischer Ventile und deren Anwendung in einem Fahrzeugdämpfer, in: *Tagungsband Mechatronik 2011*, Dresden, Germany, 2011, pp. 37–42.
- [13] H. See, Advances in electro-rheological fluids: Materials, modelling and applications, *Journal of Industrial and Engineering Chemistry* 10 (2004) 1132–1145.
- [14] M. Růžička, *Electrorheological Fluids: Modeling and Mathematical Theory*, Springer, Berlin, 2000.
- [15] K. Rajagopal, A. Wineman, Flow of electrorheological materials, *Acta Mechanica* 91 (1992) 57–75.
- [16] H. Gavin, Annular poiseuille flow of ER and MR materials, *Journal of Rheology* 45 (4) (1995) 983–994.
- [17] W. Kemmetmüller, *Mathematical Modeling and Nonlinear Control of Electrohydraulic and Electrorheological Systems*, Shaker, Aachen, Germany, 2008.
- [18] M. Whittle, R. J. Atkin, W. A. Bullough, Dynamics of an electrorheological valve, *Journal of Modern Physics B* 10 (23-24) (1996) 2933–2950.
- [19] O. Nelles, *Nonlinear System Identification*, Springer, Berlin, Germany, 2001.
- [20] K. Holzmann, W. Kemmetmüller, A. Kugi, M. Stork, Design, mathematical modeling and control of an asymmetrical electrorheological damper, in: *Proceedings CD of the 4th IFAC Symposium on Mechatronic Systems*, Vol. 4, Heidelberg, Germany, 2006, pp. 372–377.
- [21] T. Butz, O. Stryk, Modeling and simulation of electro- and magnetorheological fluid dampers, *Journal of Applied Mathematics and Mechanics* 82 (2002) 3–20.
- [22] J. Kim, Y. Cho, H. Choi, H. Lee, S. Choi, Electrorheological semi-active damper: Polyamlin based ER system, *Journal of Intelligent Material Systems and Structures* 13 (2002) 509–513.